Environmental Modelling and Software 111 (2019) 459–471

Contents lists available at ScienceDirect

Environmental Modelling & Software

journal homepage: www.elsevier.com/locate/envsoft

A linked modelling framework to explore interactions among climate, soil water, and land use decisions in the Argentine Pampas

Guillermo A. García[a,b,*], Pablo E. García[c], Santiago L. Rovere[d], Federico E. Bert[b,f], Federico Schmidt[d], Ángel N. Menéndez[c], Marcelo D. Nosetto[a,g], Andrew Verdin[h], Balaji Rajagopalan[h], Poonam Arora[i], Guillermo P. Podestá[j]

[a] *Grupo de Estudios Ambientales, Instituto de Matemática Aplicada San Luis, CONICET & Universidad Nacional de San Luis, San Luis, Argentina*
[b] *CREA Argentina, Argentina*
[c] *Laboratorio de Hidráulica, Instituto Nacional Del Agua, Ezeiza, Buenos Aires, Argentina*
[d] *Independent Scholar, Argentina*
[f] *Cátedra de Cerealicultura, Facultad de Agronomía, Universidad de Buenos Aires, Buenos Aires, Argentina*
[g] *Cátedra de Climatología Agrícola, Facultad de Ciencias Agropecuarias, Universidad Nacional de Entre Ríos, Oro Verde, Entre Ríos, Argentina*
[h] *Department of Civil, Environmental, and Architectural Engineering, University of Colorado, Boulder, CO, USA*
[i] *Department of Management, School of Business, Manhattan College, Riverdale, NY, USA*
[j] *Rosentiel School of Marine and Atmospheric Science, University of Miami, Miami, FL, USA*

ARTICLE INFO

Keywords:
Natural-human systems
MIKE SHE
Agent-based model
Agriculture
Water table
Risk management

ABSTRACT

In flat environments, groundwater is relatively shallow, tightly associated with surface water and climate, and can have either positive and negative impacts on natural and human systems depending on its depth. A linked modelling and analysis framework that seeks to capture linkages across multiple scales at the climate/water/crop nexus in the Argentine Pampas is presented. This region shows a strong coupling between climate, soil water, and land use due to its extremely flat topography and poorly developed drainage networks. The work describes the components of the framework and, subsequently, presents results from simulations performed with the twin goals of (i) validating the framework as a whole and (ii) demonstrating its usefulness to explore interesting contexts such as unexperienced climate scenarios (wet/dry periods), hypothetical policies (e.g., differential grains export taxes), and adoption of non-structural technologies (e.g., cover crops) to manage water table depth.

1. Introduction

Throughout history, water and agriculture have been closely linked (Kirsten, 2010; Smith et al., 2010). Water for food production currently exceeds all other water needs (Rosegrant et al., 2009). Most of the global food production comes from rainfed agriculture, where soil water availability depends almost exclusively on precipitation (de Fraiture and Wichelns, 2010). Rainfed agriculture holds the potential to increase food production and reduce irrigation needs, but remains particularly vulnerable to risks associated with a shifting climate (de Fraiture and Wichelns, 2010).

The region of central-eastern Argentina known as the Pampas is one of the most important rainfed grain producing areas in the world (Calviño and Monzon, 2009; Hall et al., 1992). Most of the Pampas has an extremely flat topography with regional slopes lower than 0.1% (Jobbágy et al., 2008). In such flat environments, groundwater is tightly coupled to surface water and plays a key role on the functionality of the ecosystem. Low topographic gradients and poorly developed drainage networks constrain horizontal evacuation of excess water, in turn leading to shallow water tables[1] (Fan et al., 2013). Shallow water tables (generally less than 3–5 m deep) can affect and, reciprocally, be affected by the annual field crops and pastures (or natural grasslands)

Abbreviations: SAB, Salado A Basin; WTD, water table depth; PM, Pampas Model; PI, productivity index; DSSAT, Decision Support System for Agrotechnology Transfer; LAI, leaf area index; RD, root depth; SRTM, Shuttle Radar Topographic Mission; INTA, National Agricultural Technology Institute (Argentina); SMN, National Meteorological Service (Argentina)

* Corresponding author. Grupo de Estudios Ambientales, Instituto de Matemática Aplicada San Luis, CONICET & Universidad Nacional de San Luis, Av. Italia, 1556, D5700HHW, San Luis, Argentina.

E-mail address: garciagu@agro.uba.ar (G.A. García).

[1] The water table is defined as the top of the water-saturated zone (or phreatic zone) in the soil profile.

https://doi.org/10.1016/j.envsoft.2018.10.013
Received 30 August 2017; Received in revised form 6 October 2018; Accepted 26 October 2018
Available online 27 October 2018
1364-8152/

Software availability

Name of software Pampas Model
Developers Santiago L. Rovere, Federico Schmidt, Guillermo P. Podestá, Guillermo A. García, Pablo E. García and Federico E. Bert.
Contact information Santiago L. Rovere. srovere@gmail.com
Hardware required High-end computer (i7 processor or similar, 16–32 Gb RAM and virtualization capability).
Software required Repast Simphony 2.4, Java 7, MySQL Server 5.7 and MySQL Connector J, R 3.4 and additional libraries, for running Pampas Model. MIKE-SHE 2012 (Windows 7, 8, 10), OpenSSH Server, is also required.
Programming languages Java 7, R 3.4, Visual C#.
License All software is open-source, except MIKE-SHE 2012. Users who want to run MIKE-SHE must purchase a license (https://www.dhigroup.com/).

that dominate land use in the Pampas (Nosetto et al., 2009, 2015).

Agricultural production systems in the Pampas and the associated use of land and water have undergone profound changes in recent decades (Barsky and Gelman, 2009; Satorre, 2011). These changes were propelled by complex interactions among (i) favorable economic contexts tied to higher global demand for animal protein and, increasingly, biofuels (Lamers et al., 2008; Rulli et al., 2016); (ii) cost-reducing technological innovations such as no-tillage cropping and glyphosate-resistant varieties of soybean (Caviglia and Andrade, 2010; Qaim and Traxler, 2005), and (iii) marked inter-decadal variability in precipitation (Berbery et al., 2006; Castañeda and Barros, 1994), with a steady increase in annual rainfall (particularly in spring-summer) since the 1970s (Haylock et al., 2006; Rusticucci and Penalba, 2000; Vargas et al., 2002). Because of interactions among all these drivers, field crops have expanded throughout the Pampas, displacing grasslands and pastures (Manuel-Navarrete et al., 2009; Viglizzo et al., 2011).

The observed shift from mixed crop-cattle systems to continuous agriculture has influenced the dynamics of surface and groundwater in the Pampas. As crops occupy a field only during a few months per year and often have shallower roots, they consume less water than pastures or grasslands annually (Nosetto et al., 2012, 2015). Moreover, no-tillage cropping, a widely adopted practice in the Pampas (Trigo et al., 2009), leaves the soil undisturbed and covered with stubble, possibly reducing soil evaporation, increasing infiltration and reducing runoff (Sinclair et al., 2007). Consequently, lower evapotranspiration from land use change together with increased rainfall have contributed to increase groundwater recharge, favoring the rise of water tables (Contreras et al., 2011; Viglizzo et al., 2009). As water table dynamics control the formation and expansion of free-standing water bodies (Aragón et al., 2011; Kruse et al., 2001; Scarpati et al., 2002), there is an active debate in Argentine society about the links between land use changes and a perceived increase in the frequency and magnitude of flooding events with important social and economic impacts (Kuppel et al., 2015). This work aims to contribute science-based evidence to the ongoing debate.

Our goal is to explore the couplings, interdependencies, lags, and feedbacks between (i) surface and groundwater, (ii) plausible climate scenarios (e.g., wet or dry periods), and (iii) agricultural production systems in the Pampas. Towards that goal, we have implemented a modelling and analysis framework that seeks to capture linkages across multiple scales at the climate/water/crop nexus in the Pampas. This paper describes the components of the framework and, subsequently, use it as a controlled, experimental environment to explore the impacts of various climate and land use scenarios.

1.1. The study area

The study focuses on the Salado “A” Basin (SAB, Fig. 1), located in the northwestern portion of the Salado Basin in central-eastern Argentina (Forte Lay et al., 2007). This region provides a unique environment to simulate and study linkages between climate, water, and agricultural decision-making because of (i) the strong coupling between climate variability, surface and groundwater in its flat sedimentary landscape, and (ii) observed land use changes that – together with marked climate fluctuations on multiple time scales – modulate groundwater recharge, water table depth (WTD) and flood frequency.

The SAB encompasses approximately 6.9 million ha (69,000 km^2), extending about 330 km east-west and 360 km north-south. The SAB is a sedimentary basin where soils have developed on loessic materials of loamy to sandy loam textures and are predominantly Hapludolls (Hall et al., 1992). The SAB has very flat topography and poorly developed drainage networks that constrain horizontal flows of both surface and groundwater (Viglizzo et al., 2009). The climate of the SAB is characterized as temperate sub-humid (Hall et al., 1992), with mean annual rainfall decreasing westward from 1000 to 800 mm and a mean annual potential evapotranspiration of ca. 1100 mm. Although the SAB is considered to have an isohigrous regime, the colder part of the year is relatively drier, as two thirds of annual precipitation occur during the austral spring and summer (October–March). Mean daily air temperature ranges from 8 to 10 °C during winter, to 22–24 °C in summer (SMN, 2017). As with most of the Pampas, SAB production systems moved from low-input, cattle-crop rotations to a predominantly agricultural system with more intensive use of external inputs, technology and management (Viglizzo et al., 2001). The SAB area allocated to annual grain crops increased from < 40% to > 50% since the 1960s (Viglizzo et al., 2011), and wheat was replaced by full-cycle soybean as the prevailing crop (Agroindustria, 2016).

Since colonial times, the Salado Basin has shown alternating floods and droughts that displace populations and disrupt productive activities and livelihoods for extended periods. Floods were frequent during the late 19th and early 20th centuries, a relatively wet period. In contrast, extensive droughts were more frequent during the drier 1930s-1950s (Herzer, 2003; Seager et al., 2010). Partly in response to rainfall increases since the 1970s, severe floods have occurred in the Salado Basin in 1980, 1991–93, and 2000–01 (Herzer, 2003). Floods in the western

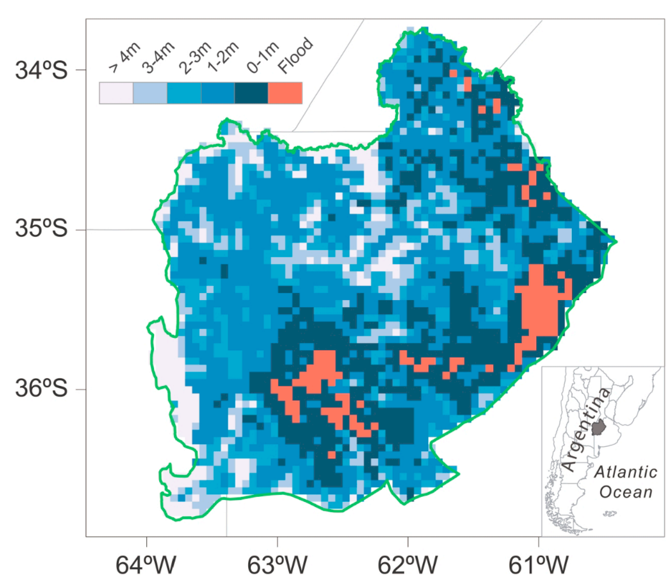

Fig. 1. Salado A Basin. The inset shows the location of the Salado A Basin in central-eastern Argentina. The cells inside the basin indicate simulated water table depth (m) for an arbitrary date. Red colors indicate free standing water (i.e., a flooded region).

half of the Pampas (mostly in the SAB) between 1997 and 2003 left more than a quarter of the landscape under water, halved grain production, damaged infrastructure and soil quality, and transformed the few remaining natural areas (Viglizzo et al., 2009). Slow floods lasting several years are characteristic of this region: they occur when the water table reaches the surface following sustained precipitation excesses (Kuppel et al., 2015). Floods in the Salado Basin not only affect rural land; long-lived flooding of urban centers has been a recurring issue in the region.

2. Linked modelling framework

2.1. Overview

We assembled a linked modelling and analysis framework to describe the reciprocal interactions and feedbacks between plausible climate scenarios, individual land use decisions, the dynamics of shallow water tables, and the emerging impacts of these interactions on regional land use, agricultural production, and the risks of floods and droughts. The various framework components and the flow of data and results among them are illustrated in Fig. 2; details on individual components are given in subsequent sections.

A major component of the framework is a fully-distributed and physically-based hydrological model used to capture the physical and biological linkages between crops, and surface and groundwater. However, production of information relevant to the science-policy dialogue also requires a thorough understanding of human choices and of the economic and social contexts in which production decisions are embedded. Because humans and their choices both influence and are influenced by the climate/water/crop nexus, we augment the biophysical models with an agent-based model of land use decisions and farm production – another major component of the framework – that includes realistic descriptions of human behavior, decision-making and social interactions. Other framework components generate necessary inputs (e.g., multiple realizations of synthetic daily weather), allow post-processing and visualization of framework results, and provide a computational environment to run large numbers of simulations relatively effortlessly.

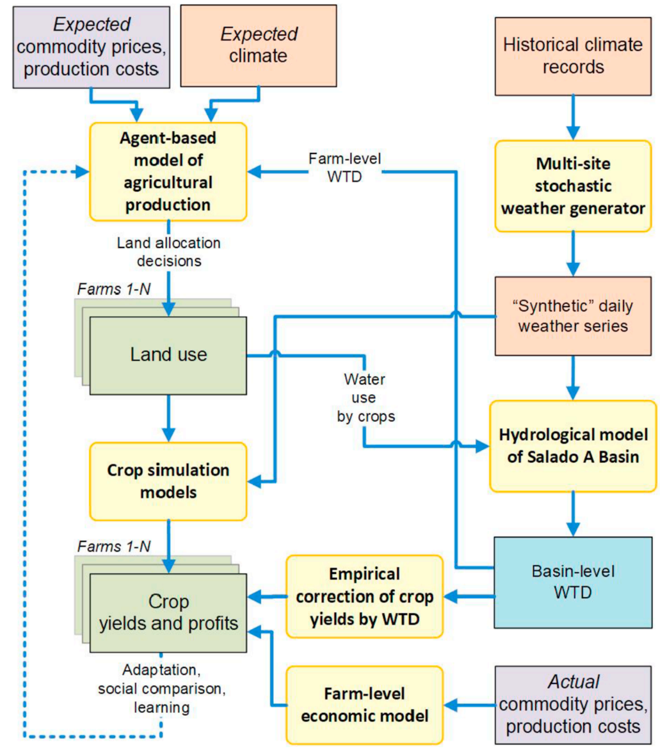

Fig. 2. Linked modelling framework. Yellow boxes indicate main components of the framework, orange boxes indicate climate inputs, purple boxes indicate economic inputs, green boxes indicate farm-level Pampas Model results, and the blue box indicates hydrological results from MIKE SHE as water table depth (WTD). Text along the lines indicates exchanges of information and results among components.

2.2. Framework components

2.2.1. The MIKE SHE hydrological model

A hydrological model of the SAB was developed using MIKE SHE, a widely-used proprietary software (Refsgaard and Storm, 1995; Refsgaard et al., 2010). MIKE SHE is a deterministic, spatially-distributed, physically-based numerical model that couples surface and groundwater flows. MIKE SHE simulates all major processes of the hydrological cycle, including evapotranspiration, overland flow, unsaturated flow, and groundwater flow (Refsgaard et al., 2010; Sahoo et al., 2006). The main link between land use decisions and the hydrological cycle is crop evapotranspiration; this process is simulated by MIKE SHE using the Kristensen and Jensen (1975) method.

Both conceptual and practical reasons justify our choice of MIKE SHE to model the SAB. Conceptually, MIKE SHE integrates all major hydrological processes into a single code and provides physically-based models for these processes. From a practical point of view, MIKE SHE has been used previously in Argentina to develop a Flood Control Master Plan for the entire Salado Basin (Badano, 2010; Menéndez et al., 2012), and recently to establish the impacts of different land uses on groundwater dynamics for the A1 sub-basin (García et al., 2017). The availability of this MIKE SHE implementation reduced significantly the start-up time for the research presented here.

For hydrological simulations, a regular grid with a horizontal spacing of 5000 m (i.e., each cell has an area of 25,000,000 m^2 = 2500 ha) was defined over the SAB and surrounding areas; about 2800 MIKE SHE cells encompass the basin. The grid spacing was chosen as a compromise between a spatial resolution sufficient to describe the processes of interest and available computer resources. A Digital Elevation Model (DEM) of the basin was based on the 90-m Shuttle Radar Topographic Mission (SRTM) data (Farr et al., 2007). Altitude shifts in the SRTM data were first corrected by fitting a third order polynomial function to elevation data provided by Argentina's National Geographic Institute, and altitudes were then averaged to the MIKE SHE 2500 ha resolution (however, the original 90 m DEM was used elsewhere). The SAB elevation decreases from 140 m.a.s.l. at the western end to about 60 m.a.s.l. in the east, a regional slope of about 0.03%. The SAB is widely covered by wind-generated depressions, where water is temporarily stored after rain events. The typical area of these depressions, however, is much smaller than the model cell size. Therefore, depressions were considered as initial water abstractions[2] from the corresponding cell.

Two main soil types with quite different properties (horizontal and vertical conductivity, saturated and residual soil moisture) were included in MIKE SHE simulations, defined as vertical profiles from the surface to a 40 m depth. Each soil was associated with a different geological formation. Three hydrogeological layers (Post-Pampeana, Pampeana and Puelche) resting on a practically impermeable layer were represented (Halcrow and Partners, 1999); details on soil types and hydrogeological layers are given in Badano (2010) and García et al. (2017). The initial condition of the unsaturated zone is established by

[2] MIKE SHE assumes a constant elevation within each 2500 ha cell. In reality, there are small scale topographic features (e.g., micro-depressions) that can hold excess water. The aggregated volume of all depressions in a cell is defined as the "initial abstraction" for that cell. Until the aggregated volume is filled, there will be no simulated surface runoff. The abstraction for each cell was estimated using a higher resolution (90 m) DEM.

an equilibrium pressure profile (resulting in a uniform WTD of 1 m across the entire basin). This relatively shallow initial WTD should be kept in mind when analyzing subsequent simulation results. Alternatively, WTD could be initialized to any desired value, but this would require an additional input grid listing initial WTD in each modeled cell.

2.2.1.1. MIKE SHE calibration in the Salado A basin. Although the MIKE-SHE model had been previously calibrated for the whole Salado Basin and other sub-basins (Badano, 2010; Menéndez et al., 2012), the model was recalibrated with specific focus on the SAB. During the calibration stage, a set of model parameters was estimated for the unsaturated zone that minimized the root mean square error (RMSE) of simulated and observed WTD time series. To reduce computation time, plausible ranges of important parameters were selected based on expert knowledge. Observed WTD was used both for calibration and validation purposes: 126 WTD series of various lengths were available; together, these series included about 14,000 individual WTD measurements. WTD values within the SAB were observed by public agencies such as the National Agricultural Technology Institute (INTA) and the National Meteorological Service (SMN), and by individual farmers. These historical WTD observations were compiled by Red MATE (a collaborative research network) and are available online (http://red-mate.agro.uba.ar/). All MIKE SHE simulations intended for calibration used as input synthetic daily weather series produced by a weather generator described in Section 3.2.3. Ten realizations of synthetic weather with statistical characteristics similar to those of observed data were produced for the period 1961–2015.

After calibration, MIKE SHE reproduced very well the observed groundwater dynamics, capturing rises and drops of the water table. As an example, Fig. 3 shows historical (red points) and simulated WTD values for three phreatimeters in different locations across the basin and covering different times spans. The gray envelope in the three panels of time series represents the WTD range for the 10 equally-likely realizations of synthetic daily weather. Two main results can be pointed out. First, observed WTDs mostly lie within the envelope of simulated values, suggesting that observed WTDs are consistent with those simulated using the synthetic weather. Second, because of the large size of a MIKE SHE cell (2500 ha), quantitative comparisons (i.e., RMSE of differences between series) of point (phreatimeter) to area (model cell) are not meaningful: MIKE SHE has a single elevation for the entire grid cell, whereas phreatimeter measurements are referred to the microrelief within a cell. Instead, we focus on assessing whether the overall trends and timing of turning points are consistent in both observed and simulated series.

2.2.2. Agent-based model of land use, the Pampas Model

Large-scale patterns (e.g., land use or WTD for the SAB) cannot be predicted from the summation of individual behaviors, as this would neglect processes such as social interactions, learning, and adaptation (Matthews et al., 2007; Schreinemachers and Berger, 2006). To address these oft-neglected processes, we used an agent-based model (Gilbert, 2008; Grimm and Railsback, 2005) to “upscale” farm-level decisions and outcomes into basin scale results (Verburg and Overmars, 2009).

The Pampas Model (PM), an agent-based model of land use decisions, was designed to understand structural changes in agricultural systems of the Pampas (Bert et al., 2010, 2011, 2014; Rovere et al., 2016). The PM considers individual decisions (e.g., land allocation, agronomic management, expansion or contraction of area cropped by a farmer) influenced by personal goals (e.g., maximization of economic utility) and characteristics (e.g., risk tolerance). Decisions are made in the context of physical (climate), economic (grain prices, costs) and social (neighbors, peer networks) conditions.

To illustrate the role of the PM within the linked framework, we briefly describe the dynamics of the model. One simulated cropping cycle represents the period from 1 May of a year to 30 April of the following calendar year. (1) At the beginning of a cropping cycle, farmers adjust their economic aspirations based on the *expected* status of context factors (i.e., climate, output prices, input costs). Then, farmers decide whether they can: (i) farm additional land (the only way to expand cropped area is by renting additional land), (ii) maintain the area cropped in the previous cycle or, instead, (iii) release some or all the previously farmed area. (2) Subsequently, farmers allocate their land among a realistic set of activities (described below). Agents may have different land allocation strategies such as imitation or maximization of an objective function (Gotts and Polhill, 2009; Gotts et al., 2003). (3) After land is allocated, the yield of each selected activity is retrieved from lookup tables that were pre-calculated using biophysical crop models (Section 3.2.4.2) and experienced climate (Section 3.2.3). A new feature introduced in the current version of the PM considers an empirical correction to grain yields based on WTD during the cycle (Section 3.2.5). Economic returns are then calculated from WTD-corrected yields and grain prices and costs specified as model inputs. The end result of the economic calculations is an updated value for the farmer's working capital at the end of the production cycle. (4) Based on achieved economic returns, farmers update their aspiration level for the following cycle (Cyert and March 1963; Lant, 1992; March, 1988). The aspiration level is a special value that separates outcomes perceived as successes or failures (Diecidue and Van De Ven, 2008), which is used as an input to decisions in the following cropping cycle. Farmers compare their economic performance to that of peers, and use that information to update their subsequent aspiration level (Herriott et al., 1985) and to imitate successful peers (Bala and Goyal, 1998).

A comprehensive validation of the PM combined (i) validation of processes and components during model development and (ii) comparison of observed and simulated results (Bert et al., 2014). The PM reproduced well observed trajectories of the number and size distribution of farms, land tenure, and land use in the Pampas (Bert et al., 2010, 2011), as well as endogenously-generated land rental prices (Bert et al., 2015). Similar validation approaches, such as expert assessment of the reasonability of outcomes simulated for specific scenarios, was used to validate the whole framework described here.

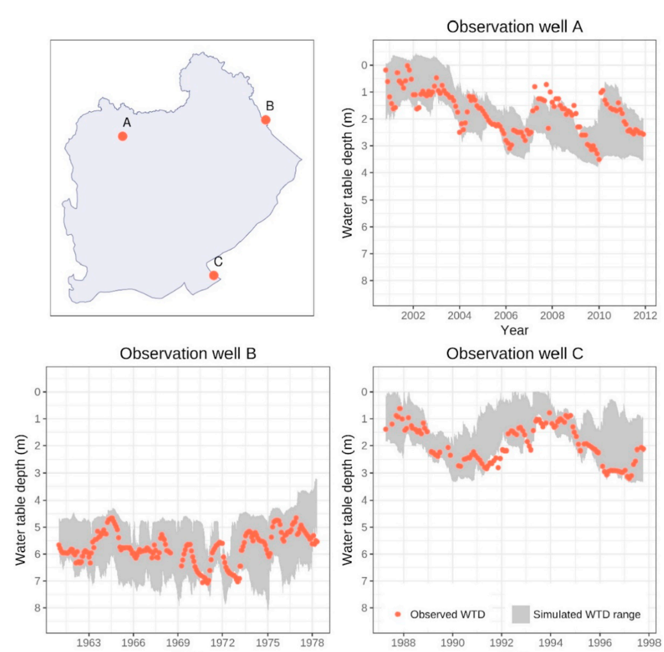

Fig. 3. Hydrological model calibration. Measured (red points) and simulated water table depth values (gray band include the 10 realizations of synthetic climate used, see Section 3.2.3) for three different observation places spatially distributed in the basin and each of them with different time windows records).

2.2.2.1. The Pampas Model's spatial environment: synthetic farms. The PM includes a spatially-explicit environment that represents the SAB. This environment contains multiple farms operated by owner or tenant agents. The overall number and size distribution of simulated farms inside the SAB environment is consistent with values reported in the 2002 Argentine Agricultural Census, which is the most recent available information on farm sizes in Argentina. Because the PM currently includes decision rules and economic calculations only for agricultural land uses, synthetic farms encompass only areas sown with annual crops.

Unfortunately, we did not have access to a cadastral map showing *actual* farm boundaries; instead, we simulated the necessary number of "synthetic farms". Briefly, the SAB was first covered with multiple tiles 20 ha in size (not to be confused with the previously-described MIKE SHE grid). Each synthetic farm was then assembled by selecting spatially contiguous tiles (whenever possible) until the desired farm area was reached. Because of this approach, all simulated farm sizes were multiples of the unit tile area. Finally, the selected tiles were then merged into one (if all tiles were contiguous) or more polygons representing the outer boundaries of a synthetic farm. Because the PM includes only agricultural decisions, simulated farms were placed only in areas apt for crop production, i.e., having soil units with a productivity index (PI; Riquier et al., 1970) ≥ 32. Note, however, that the aggregated size of synthetic farms did not completely encompass the area suitable for agriculture (PI ≥ 32). Natural grassland or implanted pasture were assumed to cover the rest of this area. Soils with PI < 32 were deemed appropriate only for cattle production; grassland or pasture were assumed to cover these soils in all simulations. A discussion of the soils used for crop modelling is presented in Section 3.2.2.2.

A total of 15,832 farms were simulated that encompassed 3,792,720 ha sown with annual crops (about 55% of the SAB). Individual farm sizes ranged between 20 and 5040 ha. The rest of the basin (3,091,181 ha, or about 45% of the SAB area) was assumed to be permanently covered by implanted or natural grasslands. Agents do not make production decisions on this land or derive profits from it, yet this land influences hydrological dynamics. The fact that about 45% of the SAB is always covered by pasture/grassland should be kept in mind when interpreting simulation results. Urban areas and roads represent a very small proportion of the SAB and thus could be safely ignored.

2.2.2.2. Pampas Model implementation in the Salado A basin: representative soils. Soil information is an input to crop simulation models. Representative soils in the SAB were defined from various sources of information. First, from a 1: 500,000 (spatial resolution) soil atlas (INTA, 1990) we identified 36 soil units (each containing 1–3 soil types) within the SAB. Of these, 19 soil types classified at subgroup level were considered apt for crop production (i.e., PI ≥ 32). Nevertheless, the atlas did not include the soil information needed for crop simulations (e.g., textural characteristics, horizon depths). To retrieve detailed soil characteristics, we relied on higher-resolution (1: 50,000) INTA soil charts that had been previously processed to be included in the Triguero® wheat simulation software (Satorre et al., 2005). From this source, 60 soil series were chosen. Some soil types were associated with only one series within the SAB, whereas the most common soils (e.g., Typic Hapludolls) included up to eight different series. When a soil type involved multiple series, crop yields were simulated for each series and then averaged.

2.2.3. A spatial stochastic weather generator

The hydrological and crop models in the linked framework require as input daily values of several weather variables on a dense spatial grid. Because of the sparse spatial distribution of weather stations in the SAB, an alternative approach to the interpolation of observed data is to drive simulations with synthetic weather series having statistical characteristics similar to those of historical data. We used the space-time weather generator developed by Verdin et al. (2018) to produce synthetic weather series on a 25 × 25 km grid encompassing the SAB – i.e., 25 MIKE-SHE grid cells (which have 5 × 5 km resolution) shared the same weather. This tool allowed us to produce synthetic series at 210 points while preserving the spatial dependence in daily weather. As multiple equally-likely weather sequences can be easily generated, this approach allows a more thorough impact assessment than use of the historical record, which represents a single realization of the weather process (Richardson, 1981). Another important feature of the weather generator is that it can accept "covariates" that can be used to mimic either observed fluctuations or to explore plausible future climate scenarios (e.g., a projected increase or decrease in rainfall, etc.).

The weather generator was trained with 1961–2015 daily data observed at 21 meteorological stations within or near the SAB and operated by SMN and INTA. We then produced 10 realizations of synthetic daily weather (maximum and minimum temperature and precipitation), each one spanning 55 years – the length of the historical climate record. Other needed quantities were estimated from the simulated variables; e.g., solar radiation was computed using the Bristow and Campbell (1984) method. To ensure consistency with historical climate in the SAB, we used three covariates: basin-wide 3-month min/max temperature averages and precipitation totals calculated from the 1961–2015 record; we refer to these series as "pseudo-historical." Last 25 years (i.e., 1990–2015) of the pseudo-historical series were used in most simulations, unless otherwise discussed.

2.2.4. Crop simulation models

Crops play two major roles in our linked modelling framework. First, crop yields directly influence the economic results achieved by farmers (other drivers such as commodity prices and input costs are kept constant) and thus have strong impact on land use decisions. Second, crops influence the hydrological system (including WTD) through their consumption of soil water.

To simulate growth, development, and yield of the main crops in the SAB – wheat (used both as harvest and cover crop), maize, soybean, and sunflower – we used models in the Decision Support System for Agrotechnology Transfer (DSSAT) package (Jones et al., 2003). DSSAT models have been previously calibrated and validated for the region (Aramburu Merlos et al., 2015; Bert et al., 2007; Grassini et al., 2009; Mercau et al., 2007; Monzon et al., 2007). The information required to run the DSSAT models includes daily weather series, soil parameters and initial conditions, crop genetic coefficients, and a description of selected crop management.

2.2.4.1. Crop simulations for MIKE SHE runs. Leaf area index (LAI, the total leaf area per unit of soil area) and vegetation root depth (RD) are inputs used by MIKE-SHE to compute actual evapotranspiration (Kristensen and Jensen, 1975). The temporal evolution of these variables for a simulation cell depends on the relative proportion of land allocated to each land use within that cell and cropping cycle. We followed several steps to estimate LAI and RD values, briefly discussed below.

First, daily values LAI and RD for soybean, maize, wheat and sunflower were simulated using DSSAT models. For each crop, we simulated 40 growth cycles using observed weather for Junín, a meteorological station inside the SAB, and a representative soil (Typic Hapludoll). The 40 simulated LAI and RD trajectories were then averaged into a single series for each variable and crop. In contrast, LAI and RD series for pastures/grasslands (these two covers were not separated) were defined using field data (Nosetto, personal communication).

To drive hydrological simulations, "weighted" LAI and RD were calculated for each MIKE SHE cell and cropping cycle. These values resulted from weighting the average LAI and RD values for each land use (i.e., each crop in a synthetic farm or areas with pasture/grassland) by the proportion of cell area occupied by that activity on a given simulation cycle. Crops within synthetic farms within a cell had either been selected by agents during PM simulations or, alternatively, prescribed as part of a particular simulation experiment (e.g., all synthetics farms were assumed to be covered by late maize). Pasture/grassland areas remained constant throughout all simulations.

2.2.4.2. Crop simulations used by the Pampas Model. The agent-based PM includes multiple mechanisms through which agents can select a given land allocation for their farm. On each cycle, a farmer allocates land among six possible agricultural enterprises: (i) a long- or (ii) short-duration cover crop not intended for harvest (Pinto et al., 2017), followed by full-cycle soybean, (iii) wheat followed by short-cycle soybean, (iv) full-cycle soybean without cover crop, and (v) early- or (vi) late-sown maize. Sunflower[3] was not among the land uses that could be selected by agents in the PM. We assumed that wheat for harvest was always followed by a short-cycle soybean sown immediately after wheat harvest; this is a very realistic assumption for the SAB. Representative agronomic management for each of these activities (Table 1) was defined in collaboration with SAB technical experts from CREA, a collaborating farmers' NGO. Table 1 also describes soil initial conditions and relevant crop managements used in DSSAT simulations.

To explore all combinations of synthetic weather series, soils and agronomic management across the spatially-dense SAB grid, a large number of crop simulations (ca. 150,000 for the whole basin) were necessary. Running these simulations interactively would have been an extremely time-consuming and error-prone task. Instead, we adapted the parallel System for integrating Impact Models and Sectors (pSIMS) developed by Elliott et al. (2014). The pSIMS framework allowed us to use high-performance computing infrastructure to run simulations that encompassed a large spatial grid, for many cropping cycles, and evaluate multiple alternative management practices (Elliott et al., 2014).

2.2.5. Adjusting crop yields and profits for the effects of shallow water tables

Despite the fact that DSSAT and hydrological models have been successfully coupled (Ma et al., 2005, 2006, 2008), the impacts of WTDs on crop yields are still not well captured by the DSSAT crop models. A necessary step, therefore, was to implement an empirical relationship to "correct" simulated crop yields for the effects of WTD. As mentioned previously, shallow water tables can have null, positive, or negative impacts on crops, depending on their depth (Nosetto et al., 2009; Zipper et al., 2015). We used field data from Nosetto et al. (2009) to parameterize the impacts of WTD (averaged over the growth cycle of a given crop) on yield. The correction factor used to account for WTD impact on simulated yields is shown as a solid red line in Fig. 4.

For each simulated land use (e.g., full-cycle soybean) two separate DSSAT simulations were run, as we needed to capture different water stress conditions. The first simulation produced a "water-limited yield" that depended on water stored in the unsaturated soil and rainfall during the crop cycle. The second simulation, in contrast, excluded water limitations (i.e., the crop was "irrigated" when soil water was insufficient) and the result was a "potential yield" (Fischer et al., 2014). Farmers often seek a compromise between maximizing profit and minimizing risk at farm scale, rather than maximizing the yield of individual crops. This behavior translates into an input usage that is economically appropriate but insufficient to maximize yields. To capture the effects of these moderate input levels, both potential and water-limited yields were multiplied by 0.8, thus obtaining "attainable" potential and water-limited yields, respectively (Aramburu Merlos et al., 2015; Sadras et al., 2015).

Four distinct WTD bands (depths vary with crops) with different impacts on crop yield were identified (Fig. 4). (1) At the bottom (Band 4), with deep water tables groundwater is not accessible to plant roots and thus it does not influence crop growth or yield. In this case, there is no correction for WTD effects (i.e., for this band there is no red line indicating the yield correction factor). The attainable yields in this band – that represent water-limited conditions – can show a wide range of values (lighter red band), as they depend on available soil water and rainfall during the cycle. These yields are simulated well by DSSAT and thus do not require empirical correction. (2) If the water table is shallower (Band 3), groundwater can reach roots through capillary rise (blue dots on the middle soil profile), thus it can provide part – but not all – of the crop water requirements (Ayars et al., 2009). This "groundwater subsidy" (Lowry and Loheide, 2010; Mejia et al., 2000; Zipper et al., 2017) reduces water limitations and moves yields of rainfed crops closer to the "potential yield", even if precipitation is insufficient (Jobbágy and Jackson, 2004; Nosetto et al., 2009). To capture WTD impacts for this band and shallower ones (i.e., Bands 1, 2 and 3), corrected yields are estimated as the product of the attainable potential yield and the correction factor. As water table is deeper along this band, the yield correction factor decreases exponentially from 1 (at the bottom of Band 2) to a value defined as the ratio between (i) water-limited and (ii) potential yields, that varies for each cropping cycle. The numerator of this ratio varies mostly with rainfall during the cycle (see range at the bottom of Fig. 4), whereas the denominator responds almost exclusively to temperature and radiation. (3) If the water table is at an optimal "Goldilocks" depth (Band 2), the groundwater compensates any rainfall deficit and the crop is not water-limited, thus the attainable potential yield can be reached (i.e., yield correction factor = 1). (4) If WTD is very shallow (Band 1), the positive effects of groundwater are replaced by a "groundwater penalty", the negative impacts of waterlogging that limits root activity, nutrient availability, and plant establishment (Kahlown and Azam, 2002; Zipper et al., 2015). The correction factor and therefore simulated yields decrease rapidly with shallower WTDs until the factor equals zero, indicating total crop loss. Finally, a tipping point occurs as the water table reaches the surface: free-standing water flows much faster than within the soil, thus spatial and temporal connectivity increases abruptly, possibly triggering large flood events.

2.2.6. Economic calculations

The WTD-corrected yields are used to compute WTD-corrected economic profits that influence farmers' decisions during the following cropping cycle (Fig. 2). Details of profit calculations are given in Bert et al. (2015); here we discuss only those calculations that were modified for this work. Variable direct costs – i.e., harvesting, marketing, and transportation costs – are a function of crop yields. Transportation costs vary with distance from farmgate to export or processing facilities. This item accounts for a large fraction of total production costs in the SAB: about 15–20% of the gross value of harvested grains. In earlier versions of the PM we had assumed an average distance to the port of Rosario (where most grain processing and export facilities are located) for each of the two regions studied. Instead, here we computed the shortest route distance from the centroid of each synthetic farm (Section 3.2.2.1) to Rosario using the Google Maps Direction Application Programming Interface (developers.google.com/maps/documentation/directions/intro).

2.2.6.1. Input/output prices. Input costs and output prices were held constant for all simulations, unless indicated otherwise. Input costs (e.g. seed, fertilizer, agrochemicals, and labors) corresponded to April–June 2015 (when inputs would have been purchased for the reference cropping cycle 2015–2016). Costs were extracted from the "Agroseries" data base (https://www.crea.org.ar/agroseries-app/) maintained by CREA. Output (grain) prices were obtained from the Rosario Board of Trade (http://www.cac.bcr.com.ar), and corresponded to those months when most of the production is traded for each crop: January–March, April–August and May–June 2016 for

[3] As the sunflower model in DSSAT – OILCROP-SUN 3.5 (98.0) – was not available for the latest DSSAT version (v4.6) compatible with pSIMS, we used an earlier version but only for MIKE SHE calibration.

Table 1
Description of possible agricultural land use decision for farmers in the Salado A Basin. Soil initial conditions and relevant crop management used in DSSAT simulations are indicated. Genotypes adapted for the region were used.

Land use	Crop	Soil initial conditions			Crop management			
		Date (doy)	Water (%ASW)	N (kg ha^{-1})	Sowing date (doy)	Sowing rate (seeds m^{-2})	N fertilization rate (kg N ha^{-1})	Herbicide as desiccant application (doy)
LCC-Sb	Wheat (cover)	121	100	50	121	330	60	295
	Soybean	304	40	40	305	28	–	–
SCC-Sb	Wheat (cover)	121	100	50	121	330	50	253
	Soybean	304	75	40	305	28	–	–
Wh-Sb	Wheat (grain)	121	100	50	166	330	80	–
	Soybean	343	54	40	344	32	–	–
EaMz	Maize	121	100	60	263	7	90	–
LaMz	Maize	121	100	80	335	6	60	–
Sb	Soybean	121	100	60	305	28	–	–

doy: day of the year; ASW: available soil water; LCC: long cover crop; SCC: short cover crop; Sb: soybean; Wh: wheat; EaMz: early maize; LaMz: late maize.

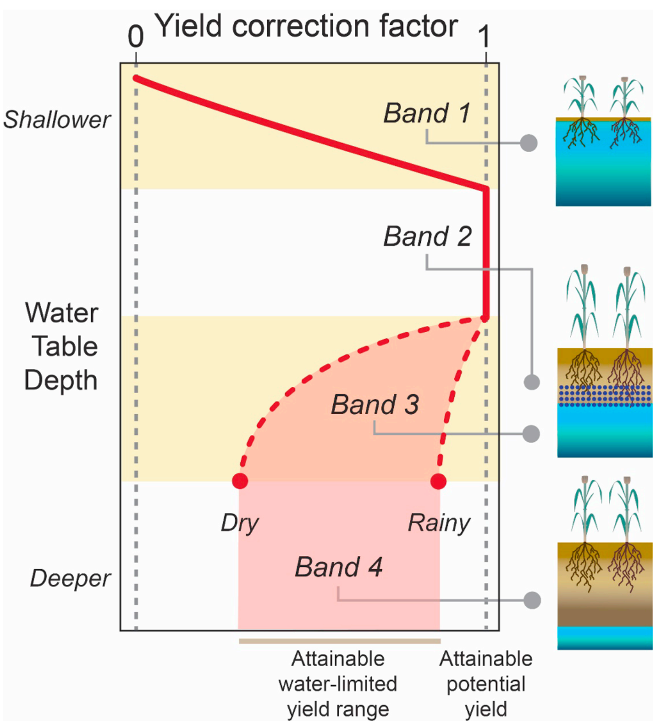

Fig. 4. Empirical correction factor for water table depth (WTD) effects on simulated crop yield. The curve was parameterized with field data from Nosetto et al. (2009). The optimal WTDs (Band 2) for wheat, maize and soybean yields were 0.7–1.4 m, 1.4–2.4 m and 1.2–2.2 m, respectively. The correction factor is a function of WTD averaged during each crop's growing cycle: May–November (wheat), September–February (early-sowing maize), November–April (late-sowing maize), October–March (full-cycle soybean) and December–April (short-cycle soybean).

wheat, maize and soybean, respectively. All values were expressed in April–June 2015 US dollars (USD) using US Bureau of Labor Statistics "All Commodities" series (https://download.bls.gov/pub/time.series/wp/wp.data.1.AllCommodities). Exchange rates from Argentine pesos (ARS) to USD were obtained from Argentina's Central Bank (http://www.bcra.gov.ar/).

2.3. Flow of information among framework components

The various components of the linked modelling framework (Fig. 2) must be able to exchange information and results throughout the simulations. Some inputs are defined during the setup and initialization stages: for instance, synthetic weather and crop yields (water-limited or not) are simulated at the beginning of an experiment and results are accessed when needed. As the simulations iterate over the desired number of simulated cropping cycles, data flow among framework components: the results of one component become inputs to another component. For brevity, we focus on the flows between the two main components of the framework: the land use PM and the hydrological MIKE SHE model.

At the start of a cropping cycle, PM agents select land allocation within their farms. This information is then processed into inputs needed by MIKE SHE: time series of weighted LAI and RD for each model cell (Section 3.2.4.1). Note that these series include the pasture/grassland area within a MIKE SHE cell but not included in farmers' allocation decisions. Once this information is passed, the PM pauses while MIKE SHE simulates hydrological processes. Synthetic weather (Section 3.2.3) for the cycle being simulated is retrieved from netCDF files and converted into the DFS2 input format supported by MIKE SHE. The hydrological model produces a daily time series of WTD for each cell and for the cropping cycle being simulated. These series are stored in another netCDF file and passed back to the PM, where an average WTD for each crop's growing cycle is computed for each farm in order to calculate WTD-corrected yields and economic results. Note that both the empirical correction of yields for WTD effects and farm-level economic calculations are discussed as individual components and shown separately in Fig. 2 to facilitate presentation, but they are actually implemented within the PM. The PM then updates the working capital for each simulated farmer and the following simulation cycle begins.

There are standard interfaces that allow the exchange of information between two or more model components and the intercommunication of processes running on different platforms: an example is the OpenMI interface (http://www.openmi.org/). To use this interface, however, each component involved must be compliant with the protocol defined by OpenMI. The MIKE SHE version to which we had access – v. 2012 for Windows – was not OpenMI-compliant; this capability became available for later versions. In contrast, as the PM was entirely developed by us in Java, it would have been possible to implement the OpenMI protocol.

As we were unable to use the OpenMI standard, we implemented an ad-hoc protocol to exchange information between framework components that was based on intermediate files in the formats needed by the component receiving each input. This was an acceptable alternative in the context of the current framework because exchanges are fairly limited – flow of data between the PM and MIKE SHE occurs only once in each direction during a simulated cropping cycle. As more complex functionalities are added – e.g., the ability by farmers to modify decisions in response to WTD *at various times* during a cropping cycle – several starts and stops of hydrological and agronomic management simulations will be required, with multiple exchanges of information during a cycle.

2.4. Validation of the entire linked modelling framework

Our linked framework includes components that already had been separately validated, showing their capacity to reproduce important patterns of the systems each model represents. The MIKE SHE hydrological model had been validated earlier for the entire Salado Basin (Badano, 2010; Menéndez et al., 2012), and recalibrated/validated for the A1 sub-basin (García et al., 2017, 2018) and the SAB (Section 3.2.1.1). Similarly, the land use agent-based model PM also had undergone a thorough previous validation that combined conceptual and empirical approaches (Bert et al., 2014).

In contrast, validation of the linked framework described here – i.e., the process of assessing the level of confidence that can be placed in the framework's overall results – is more difficult. The framework involves multiple models describing the dynamics of the target coupled natural and human systems. Such integrative frameworks almost invariably involve non-linearities, stochastic dynamics and micro-macro feedback loops (Fagiolo et al., 2007). The ability to replicate empirical evidence is often seen as the only truly decisive criterion for quality of a scientific model. However, most integrative frameworks are used to explore interesting scenarios for which there are no real-world data available. Indeed, many of the data needed both as inputs and to compare the recent historical trajectory of the target systems with simulated results were unavailable.

For the reasons discussed above, we adopted a conceptual validation approach for the framework. First, we sought to ensure that all framework components involved reasonable real-world mechanisms and properties: this process is what Rand and Rust (2011) call “microface validation.” Secondly, we followed the TAPAS (Take A Previous Model and Add Something) approach (Frenken, 2006; Polhill et al., 2010). This incremental approach enhances the conceptual validity of new or newly-linked models by building upon previously used and accepted models, components and underlying assumptions. Finally, overall framework validity can be enhanced through the POM (Pattern-Oriented Modelling) approach proposed by Grimm et al. (2005). The central idea behind POM is using patterns observed in real systems, such as the recent rise in shallow water tables, to guide the design of model structure and check whether the expected patterns are produced.

3. Climate, hydrology, and land use interactions in the pampas

This section presents results from simulations performed with the linked modelling framework with the twin goals of (i) validating the framework as a whole and (ii) demonstrating its usefulness to explore interesting contexts such as unusual climate scenarios (e.g., multi-annual wet/dry sequences), hypothetical policies (e.g., differential export taxes on agricultural commodities), and adoption of non-structural technologies (e.g., cover crops) to manage WTD. Simulated experiments are organized into three groups: results for the various groups range from quite predictable *a priori* by experts (and thus used for conceptual validation), to relatively unpredictable emerging patterns (used to demonstrate the usefulness of the framework). Simulated contexts represent both realistic and less realistic scenarios, but do not necessarily correspond to any observed situation.

3.1. Combining land use and climate scenarios

The first group of experiments was intended to provide face validation of the framework by exploring whether relatively extreme scenarios of land use and climate produced WTD patterns anticipated by regional experts. In flat environments such as the SAB, groundwater recharge mostly depends on rainfall, whereas groundwater discharge is mainly modulated by vegetation (Jobbágy and Jackson, 2004; Jobbágy et al., 2008; Viglizzo et al., 2009). To simulate the interactions between these two drivers, we ran seven experiments: in each one, a single land use (the six agricultural uses considered in the PM plus pasture) were assigned to the whole agricultural area in the SAB (i.e., about 55% of the basin). The remaining portion of the SAB (i.e., 45%) was always assigned to pasture/grassland. Each of these seven land uses was simulated with three different climate scenarios: dry, normal, and wet climate.

These experiments did not involve the long pseudo-historical climate series used in all other simulations. Instead, we created three *ad hoc* sets of daily weather series, two of which were fairly extreme and the third represented normal conditions. The climate scenarios were created as follows. First, we picked the weather realization (out of the 10 we had simulated) with the highest range of May–April precipitation values over 54 cropping cycles. For this realization, we sorted all May–April precipitation totals in ascending order. The 15 cycles with lowest totals represented the “dry” weather *ad hoc* scenario. Similarly, the “wet” *ad hoc* scenario included those 15 cropping cycles with the highest rainfall totals. The remaining 24 cropping cycles were considered as the “normal” *ad hoc* scenario. Cropping cycles within each scenario were randomly shuffled to avoid systematic patterns (e.g., temporally-increasing rainfall). Annual rainfall totals (averaged over the SAB) for the dry, normal, and wet scenarios were about 700, 950, and 1200 mm cycle^{-1}, respectively. All 21 combinations of weather and land use were run through the framework (crop selection by individual agents was disabled and land use was externally imposed). In all scenarios, initial WTD was set at -1 m.

The combined effects of (i) cropping cycle rainfall in the three scenarios and (ii) total water consumed by crops and pastures were reflected in fairly different temporal WTD patterns (Fig. 5). As

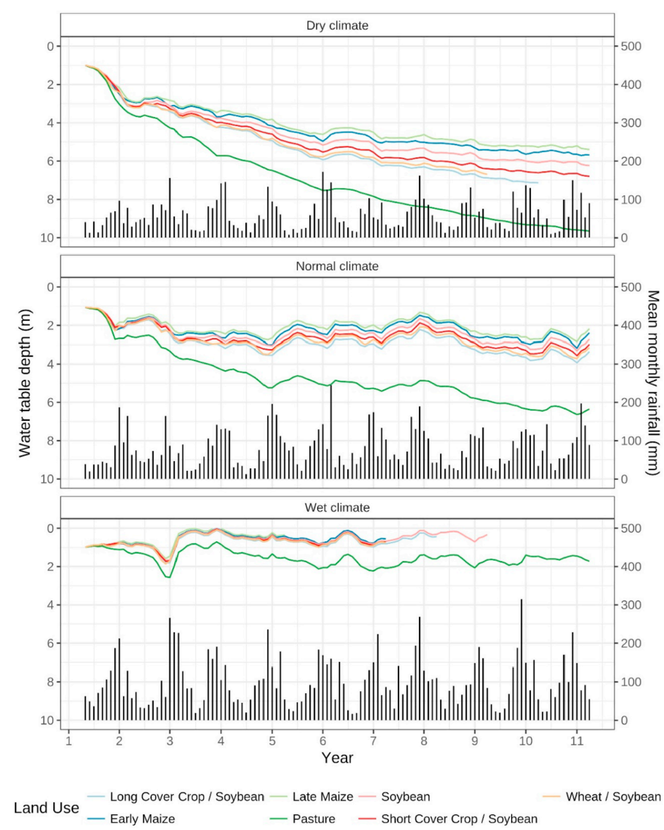

Fig. 5. Climate and land use decision influence on water table depth (WTD). Temporal variation of the in basin-wide average WTD for the Salado A Basin where farmers allocated the same land use to the whole agricultural area (ca. 55% of the basin, area with non-agricultural aptitude is always covered by pasture or natural grassland) under three *ad hoc* synthetic climate series which varied in cumulative annual rainfall – black bars indicate mean monthly rainfall. Shorter WTD series (e.g. wheat/soybean in dry climate) are a consequence of all farmers in the basin leaving production due to poor economic outcomes.

expected, the water table was deeper when the basin was covered with pasture, as this use consumes water throughout the entire cropping cycle and has deeper roots than grain crops (Nosetto et al., 2015). When the SAB was fully covered with pasture, the water table was at least 1 m deeper (in the "wet" scenario) than for all agricultural land uses. WTD differences between crops and pasture were larger for both "dry" and "normal" climates although, as expected, WTDs were shallower in the latter scenario. Among agricultural land uses, double crops induced deeper water tables than single crops. These differences, however, were only apparent under "dry" or "normal" *ad hoc* climates, and almost negligible in the "wet" *ad hoc* climate. The six agricultural land uses can be ordered by the temporal evolution of WTD that they induced. From shallower to deeper WTD this order was: late-sowing maize, early-sowing maize, full-cycle soybean, short cover crop + soybean, wheat/soybean, and long cover crop + soybean. Shorter WTD series for some agricultural land uses observed under extreme climates (e.g. wheat/soybean in "dry" climate) are a consequence of all farmers in the basin exiting production due to poor economic outcomes.

A higher consumption of available soil water over the whole cropping cycle explains the deeper water tables under long cover crop + soybean in comparison with wheat/soybean. Soybean yield, and in turn water use, is lower when the crop is part of a double-cropping use due to its delayed sowing date (i.e., less time to evapotranspirate) and the resource depletion caused by the precedent wheat (harvest) crop (Andrade et al., 2015). The wheat/soybean double crop also has little water consumption during the transition between crops (because of low leaf area) in early summer, when high atmospheric evaporative demand occurs (Mercau et al., 2016). On the contrary, when wheat is used as cover crop, the land is released earlier, allowing an earlier sowing and establishment of the following soybean crop (by about one month, Table 1). In this case, differences in yield potential and water consumption between single or cover-following soybean are smaller or negligible (Caviglia and Andrade, 2010; Rimski-Korsakov et al., 2015).

Intra-basin variability (e.g., topography and soil aptitude) are captured by the linked modelling framework, reflecting spatial differences in the influence of climate and land use decisions on WTD. As an example, Fig. 6 shows WTD at the end of the 4th simulated cropping cycle for nine combinations of land use and climate scenarios. The impacts of land use on WTD can be explored in Fig. 6. Basin-wide average WTD increases as land use goes from late-sowing maize, to a long cover crop + soybean, to pasture. For each land use, *ad hoc* climate scenarios ranging from "dry" (top row) to "wet" (bottom row) are tied to increasingly shallower WTDs. Additionally, basin flooded area (i.e., WTD above the surface) grows from almost non-existent for pasture cover and "dry" climate (Fig. 6, upper right) to a large proportion of the SAB when late-sowing maize and "wet" climate are simulated (Fig. 6, lower left).

3.2. Influence of grain price on land use decisions and water table dynamics

Land use allocation is influenced by both internal and external drivers. Grain prices are a major driver of land use decisions by farmers in the Pampas (Calviño and Monzon, 2009; Satorre, 2011). We used the linked modelling framework to explore the implications of plausible changes in prices of agricultural commodities on (i) land use decisions influenced by the relative profitability of alternative land uses, and, in turn, (ii) water table dynamics. National market policies applied at the end of the 2000s discouraged wheat sowing in Argentina and induced an increase in the area allocated to full-cycle soybean. The most noticeable drop of wheat sowing area occurred during 2007–2013, from ca. 6 to 3.2 million ha (Agroindustria, 2016). As wheat is most often followed by a short-cycle soybean (i.e., wheat is seldom sown as a single crop in a cropping cycle), this pattern led to a smaller area allocated to double crops in the SAB, in turn, double crops were shown to have a larger influence on WTD than single crops (Fig. 5). For these experiments, we chose to vary wheat prices to influence the area assigned to the wheat/soybean double crop. Although based on historical events, these simulations do not aim to reconstruct specific historical patterns.

Wheat price for the 2015–16 cycle (140 USD ton^{-1}) was reduced by 23% (to mimic the export tax rate used by an earlier Argentine administration) and, reciprocally, increased by 23%. These two manipulations resulted in wheat/soybean price ratios of 0.37 (a low ratio) and 0.59 (a value close to the historical ratio), respectively. These wheat prices, as well as those of other grain crops (151 and 293 USD ton^{-1} for maize and soybean, respectively) and input prices were kept constant during the simulated period. The initial allocation of agricultural land in farms within the SAB was set at 1/3 of wheat/soybean, 1/3 of full-cycle soybean, 1/6 of early-sowing maize and 1/6 of late-sowing maize. The pseudo-historical climate series was used for these simulations.

The higher wheat price induced a large proportion of area sown with wheat/soybean: after 25 cropping cycles, this land use expanded from 33.3% to ca. 82% of the SAB agricultural area (Fig. 7). A low wheat price, in contrast, caused the wheat/soybean area to drop from 33.3% to less than 6% after 25 simulated cycles. For this scenario, full-cycle soybean area increased from 33.3% to about 78%. For both wheat price scenarios, farmers' adoption of cover crops was practically negligible. Admittedly, the ecological services provided by cover crops – including flood control – were not explicitly quantified within the PM, thus for the model they only incurred costs.

As expected given the results of the previous group of simulations (Fig. 5), the larger proportion of wheat/soybean induced deeper water tables in the SAB (Fig. 8). After 25 cropping cycles, the most frequent WTDs were 3.5 m in the high wheat price scenario (in response to an increased wheat/soybean area) vs. 1.3 m in the low price one (reduced

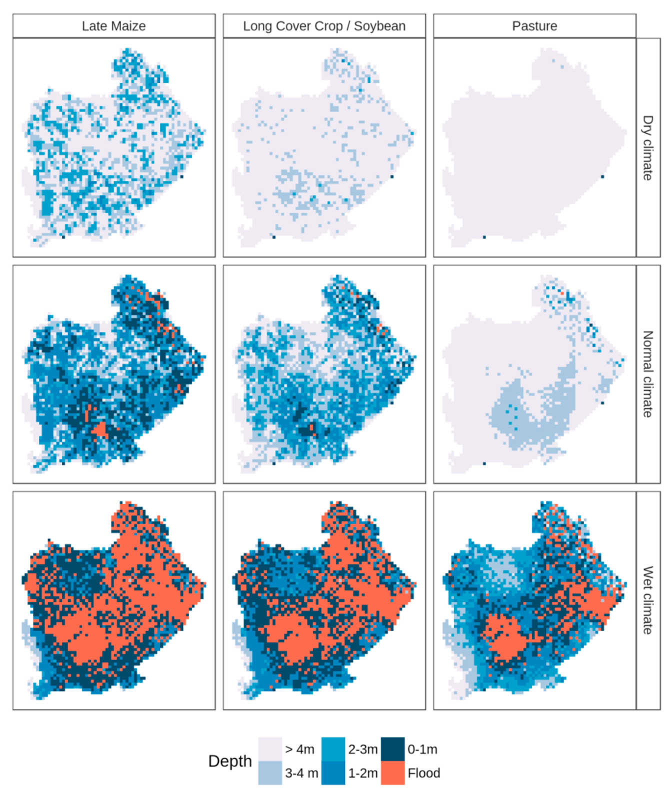

Fig. 6. Climate and land use decision influences on water table depth (WTD). Spatial variation of the WTD in the Salado A Basin where farmers allocated the same land use to the whole agricultural area (ca. 55% of the basin, area with non-agricultural aptitude is always covered by pasture or natural grassland) under three *ad hoc* synthetic climate series which varied in cumulative annual rainfall. Data correspond to the end of the fourth simulated cropping cycle.

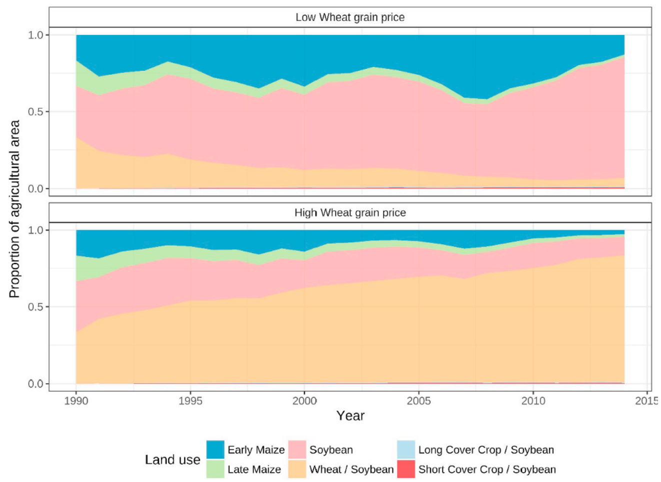

Fig. 7. Influence of grain price on land use decision. Temporal evolution of agricultural land use allocation in the Salado A Basin (proportion of the agricultural area) under different wheat grain prices, low (wheat-soybean prices ratio of 0.37, upper panel) or high (wheat-soybean prices ratio of 0.59, lower panel). Adoption of cover crops by farmers is negligible in both cases.

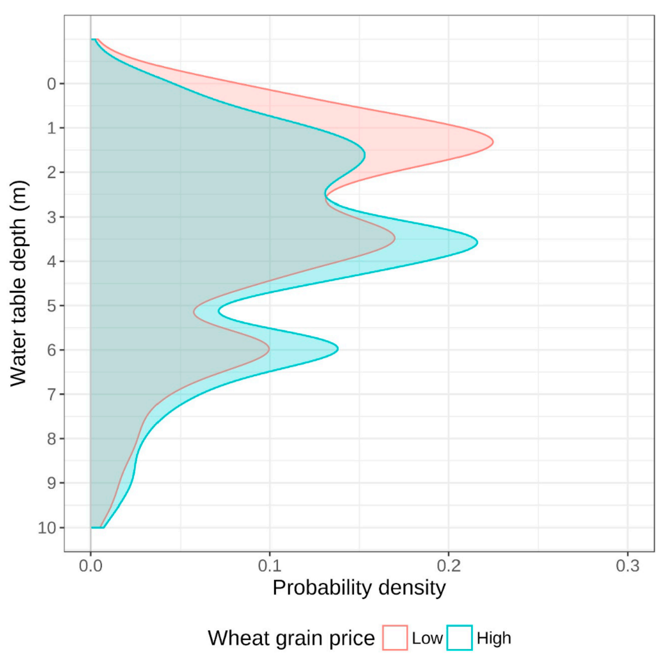

Fig. 8. Water table depth (WTD) in the Salado A Basin with different wheat grain prices. Probability density curves of WTD after 25 cropping cycles with low (wheat-soybean prices ratio of 0.37) or high (wheat-soybean prices ratio of 0.59) wheat grain prices.

wheat/soybean area). Differences between price scenarios in basin-wide average WTD began to be noticeable after 8–9 cropping cycles (data not shown).

3.3. *Can adoption of cover crops help maintain the water table at a safe depth?*

Drainage infrastructure (channels, reservoirs) have a fairly localized impact in the SAB due to the flat relief (Menéndez et al., 2012). Moreover, although often promoted as an alternative for bio-drainage (Alconada Magliano et al., 2009), forestation is infrequent in the SAB because of its slower return on investment and lack of market or business structures. Finally, as described above, the area allocated to pasture (with higher annual water consumption) has steadily decreased

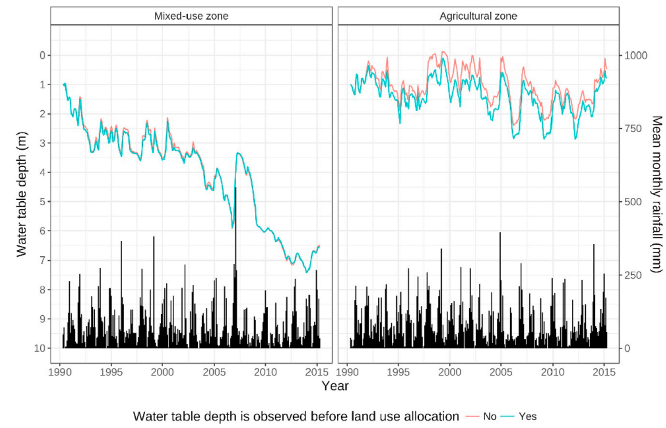

Fig. 9. Influence of cover crop adoption on water table depth (WTD) in zones (i.e., 2500 ha grid cell) with different proportion of agricultural area. Temporal variation of the average WTD when farmers consider WTD to select their land use allocation or not, in “mixed-use” (only 28% with grain crops, left panel) or “agricultural” (100% with grain crops, right panel) zones of the Salado A Basin. Mean monthly rainfall is also specified. The x-axis indicates years in the pseudo-historic climate series.

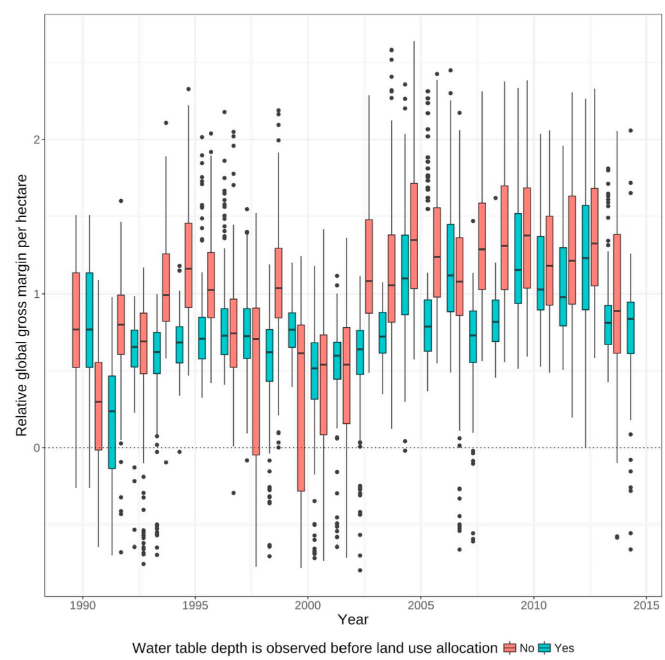

Fig. 10. Influence of cover crop adoption on agriculture economic results. Box plots of annual global gross margin per ha, relative to Salado A Basin median, when farmers consider water table depth to select their land use allocation or not. Results refers to all farms included in all “agricultural” zones (i.e., 2500 ha grid cells with 100% of the area apt for grain crops) of the basin. The x-axis indicates years in the pseudo-historic climate series.

(Viglizzo et al., 2011). For all these reasons, the choice and management of agricultural crops to help manage WTD dynamics deserves close attention (Florio et al., 2015; Mercau et al., 2016). The use of cover crops is proposed as a non-structural approach to increase soil water consumption and thus lower or prevent further rise of a shallow water table. In addition, cover crops provide many other useful ecosystem services (Pinto et al., 2017; Rimski-Korsakov et al., 2015; Schipanski et al., 2014) and many farmers are increasingly adopting them. This last group of simulations, therefore, aims to provide evidence to the debate on the use of cover crops to maintain the water table at a safe depth.

This experiment included two scenarios in which farmers either (i) do not consider or (ii) consider WTD to select their land use allocation. In the first scenario, farmers choose land uses through different mechanisms such as imitation or maximization of an objective function (Section 3.2.2), *without* considering the status of WTD. In contrast, in the second scenario farmers observe WTD in their farms on May 1st (the beginning of a cropping cycle) and act according to the following rules: (i) if WTD is deeper than 2 m, farmers follow their usual land allocation mechanism; (ii) if, on the other hand, WTD is shallower than 2 m (suggesting the potential for waterlogging and flooding) farmers ignore their land allocation mechanism and, instead, sow a long cover crop followed by full-cycle soybean. Constant input and output prices and pseudo-historical climate series were used in both scenarios. It is important to highlight that the strategy explored is only one of several plausible rules. Recommendation of land use decisions is not an objective of this work. Instead, we aim to illustrate the usefulness of the linked modelling framework to explore complex problems such as this.

As shown above (Figs. 5 and 6), simulated WTD for each 2500 ha grid cell in the framework domain is influenced by the type and proportion of land use in that cell (Section 3.2.1). Fig. 9 shows time series of WTD in two model cells with different covers: (i) a "mixed-use" zone in which only 28% of the area was apt for grain crops and the rest was assumed to be covered by pasture/grassland, and (ii) an "agricultural" zone in which the entire cell was covered by grain crops. Both cells have similar precipitation totals (ca. 1000 mm) and annual distribution. For each type of cover, Fig. 9 displays WTDs simulated with and without considering WTD as part of land use selection.

In a "mixed-use" zone (Fig. 9, left panel), WTDs decrease steadily throughout the simulation, and thus are not expected to present significant risks. In this situation, cover crop adoption is not very relevant (from a hydrological perspective). In fact, conditions leading to cover crop use occurred only once (during the first year of simulation, as WTD was initialized at 1 m depth). In the "agricultural" zone, in contrast, simulated WTDs were shallower than 2 m during a large portion of the simulation. Consequently, farmers who based land use decisions on WTD sowed cover crops in most years. Cover crop use helped maintain water tables about 0.4 m deeper than without cover crops. At the same time, the use of cover crops lowered the probability of WTDs reaching very risky levels (< 0.5 m) from 21% to about 2%.

As we only consider the hydrological implications of the use of cover crops (the current model does not quantify their other ecological services), it seems appropriate to focus on situations in which a shallow water table creates high risks of waterlogging and flooding, i.e., when land is covered by crops. We selected all cells within the model domain that had 100% agricultural cover and calculated economic results (relative to the basin's median) for every farm inside those cells for both experimental scenarios, that is, considering WTD to allocate land (Fig. 10, blue boxes and whiskers) and not considering WTD (Fig. 10, red boxes and whiskers).

In most cropping cycles, the use of cover crops to maintain water table at a safe depth resulted in somewhat lower average profits but with a considerably lower dispersion (i.e., much less variable profits) than when cover crops were not used. On average for the entire simulation, the relative global gross margin (no units) obtained by farmers willing to use cover crops was 0.79 ± 0.43 vs. 0.97 ± 0.57 for those who did not monitor WTD and thus never used cover crops. In this experiment, negative results (i.e., relative global gross margin ≤ 0) were more frequent for farmers who did not consider WTD in their land use decision (7% of the cases vs. 4% by farmers who adopted cover crops in response to shallow WTD).

The patterns of relative profitability respectively associated with use/no use of cover crops could have several explanations. First, cover crops imply higher costs but produce no income as they are not harvested, thus average profits are lower. A second reason for this result could be that in dryer years cover crops lower the WTD and therefore eliminate the groundwater subsidy for the soybean that follows. At the same time, avoidance of extremely shallow WTDs for which total losses were possible may have contributed to the higher stability of profits. Stability of economic results is an issue that has great relevance for small farmers, as one or two consecutive years of negative profits may cause small farmers to run out of working capital and exit production (Bert et al., 2011).

4. Concluding remarks

Soil water is a major link between climate, food and energy production, and other agroecosystems services (Jobbágy and Jackson, 2004; Zipper et al., 2015). This work described a linked modelling and analysis framework intended to capture linkages across multiple scales at the climate/water/crop nexus in an extremely flat environment such as the Argentine Pampas. Various groups of experiments were performed to both validate the framework as a whole (individual components had been validated previously) and to demonstrate the usefulness of the linked framework to address complex problems involving both natural and human dimensions.

First, we explored the combined effects of cropping cycle rainfall under contrasting *ad hoc* climate scenarios (e.g., wet/normal/dry) and total water consumed by different land uses (various crops and pasture). As expected, the various combinations of land use and climate resulted in fairly different temporal and spatial patterns of WTD across the SAB. The impact of fluctuations in relative grain prices on selected land use and, in turn, on water table dynamics was also captured by the linked modelling framework. Finally, we explored the adoption of nonstructural approaches to manage WTD, such as the use of cover crops. In agricultural systems where shallow water tables create recurrent risks of waterlogging and flooding, winter cover crops can be used to keep water tables at a safe depth.

Acknowledgements

This research was supported by the National Science Foundation (NSF, USA) grant 1211613 (Dynamics of Coupled Natural and Human Systems), by the Inter-American Institute for Global Change Research (IAI) grant CRN-3035 (The IAI is supported by the NSF grant GEO-1128040), by the National Agency for Science and Technology Promotion (ANPCyT, Argentina) grant PICT 2790/14, and by the National Scientific and Technical Research Council (CONICET, Argentina) grant PIP 112-201501-00609. GAG held a postdoctoral fellowship from CONICET. Climate data were kindly provided by the Regional Climate Centre for Southern South America.

References

Agroindustria, 2016. Datos Abiertos Agroindustria (Public Data). Production/Estimates. Ministerio de Agroindustria, Presidencia de la Nación, Buenos Aires, Argentina 2016. https://datos.magyp.gob.ar/reportes.php?reporte=Estimaciones.
Alconada Magliano, M.M., Bussoni, A., Rosa, R., Carrillo Rivera, J.J., 2009. El bio-drenaje para el control del exceso hídrico en Pampa Arenosa, Buenos Aires, Argentina. Invest. Geográficas 50–72.
Andrade, J.F., Poggio, S.L., Ermácora, M., Satorre, E.H., 2015. Productivity and resource use in intensified cropping systems in the Rolling Pampa, Argentina. Eur. J. Agron. 67 (0), 37–51.
Aragón, R., Jobbágy, E.G., Viglizzo, E.F., 2011. Surface and groundwater dynamics in the sedimentary plains of the Western Pampas (Argentina). Ecohydrology 4 (3), 433–447.
Aramburu Merlos, F., Monzon, J.P., Mercau, J.L., Taboada, M., Andrade, F.H., Hall, A.J., Jobbagy, E., Cassman, K.G., Grassini, P., 2015. Potential for crop production increase in Argentina through closure of existing yield gaps. Field Crop. Res. 184, 145–154.
Ayars, J.E., Shouse, P., Lesch, S.M., 2009. In situ use of groundwater by alfalfa. Agric. Water Manag. 96 (11), 1579–1586.
Badano, N., 2010. Modelación integrada de grandes cuencas de llanura con énfasis en la evaluación de inundaciones. Facultad de Ingeniería. Universidad de Buenos Aires, Buenos Aires, Argentina, pp. 158.
Bala, V., Goyal, S., 1998. Learning from neighbours. Rev. Econ. Stud. 65, 595–621.
Barsky, O., Gelman, J., 2009. Historia del agro argentino: desde la conquista hasta fines del siglo XX, third ed. Sudamericana, Buenos Aires.
Berbery, E.H., Doyle, M.E., Barros, V., 2006. Tendencias regionales en la precipitación. In: Barros, V., Clarke, R., Silva Días, P. (Eds.), El cambio climático en la Cuenca del Plata, first ed. CIMA-CONICET, Buenos Aires, pp. 61–73.

Bert, F., North, M., Rovere, S., Tatara, E., Macal, C., Podestá, G., 2015. Simulating agricultural land rental markets by combining agent-based models with traditional economics concepts: the case of the Argentine Pampas. Environ. Model. Software 71, 97–110.
Bert, F.E., Laciana, C.E., Podesta, G.P., Satorre, E.H., Menéndez, A.N., 2007. Sensitivity of CERES-Maize simulated yields to uncertainty in soil properties and daily solar radiation. Agric. Syst. 94, 141–150.
Bert, F.E., Podestá, G.P., Rovere, S., González, X., Menéndez, A., Ruiz Toranzo, F., Torrent, M., North, M., Macal, C., Sydelko, P., Weber, E.U., Letson, D., 2010. Agent based simulation of recent changes in agricultural systems of the Argentine Pampas. Adv. Appl. Statistic. Sci. 2 (2), 213–231.
Bert, F.E., Podestá, G.P., Rovere, S.L., Menéndez, Á.N., North, M., Tatara, E., Laciana, C.E., Weber, E., Toranzo, F.R., 2011. An agent based model to simulate structural and land use changes in agricultural systems of the argentine pampas. Ecol. Model. 222 (19), 3486–3499.
Bert, F.E., Rovere, S.L., Macal, C.M., North, M.J., Podestá, G.P., 2014. Lessons from a comprehensive validation of an agent based-model: the experience of the Pampas Model of Argentinean agricultural systems. Ecol. Model. 273 (0), 284–298.
Bristow, K.L., Campbell, G.S., 1984. On the relationship between incoming solar radiation and daily maximum and minimum temperature. Agric. For. Meteorol. 31 (2), 159–166.
Calviño, P., Monzon, J., 2009. Farming systems of Argentina: yield constraints and risk management. In: Sadras, V., Calderini, D. (Eds.), Crop Physiology. Academic Press, San Diego, pp. 55–70.
Castañeda, M.E., Barros, V., 1994. Las tendencias de la precipitación en el Cono Sur de América al este de los Andes. Meteorológica 19 (1–2), 23–32.
Caviglia, O.P., Andrade, F.H., 2010. Sustainable intensification of agriculture in the Argentine Pampas: capture and use efficiency of environmental resources. Am. J. Plant Sci. Biotechnol. 3 (Special issue 1), 1–8.
Contreras, S., Jobbágy, E.G., Villagra, P.E., Nosetto, M.D., Puigdefábregas, J., 2011. Remote sensing estimates of supplementary water consumption by arid ecosystems of central Argentina. J. Hydrol. 397 (1–2), 10–22.
Cyert, R.M., March, J.G., 1963. A Behavioral Theory of the Firm. Prentice-Hall, Englewood Cliffs, NJ.
de Fraiture, C., Wichelns, D., 2010. Satisfying future water demands for agriculture. Agric. Water Manag. 97 (4), 502–511.
Diecidue, E., Van De Ven, J., 2008. Aspiration level, probability of success and failure, and expected utility. Int. Econ. Rev. 49 (2), 683–700.
Elliott, J., Kelly, D., Chryssanthacopoulos, J., Glotter, M., Jhunjhnuwala, K., Best, N., Wilde, M., Foster, I., 2014. The parallel system for integrating impact models and sectors (pSIMS). Environ. Model. Software 62, 509–516.
Fagiolo, G., Moneta, A., Windrum, P., 2007. A critical guide to empirical validation of agent-based models in economics: methodologies, procedures, and open problems. Comput. Econ. 30 (3), 195–226.
Fan, Y., Li, H., Miguez-Macho, G., 2013. Global patterns of groundwater table depth. Science 339 (6122), 940–943.
Farr, T.G., Rosen, P.A., Caro, E., Crippen, R., Duren, R., Hensley, S., Kobrick, M., Paller, M., Rodriguez, E., Roth, L., Seal, D., Shaffer, S., Shimada, J., Umland, J., Werner, M., Oskin, M., Burbank, D., Alsdorf, D., 2007. The Shuttle radar topography mission. Rev. Geophys. 45 (2) (n/a-n/a).
Fischer, R.A., Byerlee, D., Edmeades, G.O., 2014. Crop Yields and Global Food Security: Will Yield Increase Continue to Feed the World? ACIAR Monograph No. 158. Australian Centre for International Agricultural Research, Canberra, Australia, pp. 634.
Florio, E.L., Mercau, J.L., Nosetto, M.D., 2015. Factores que regulan la dinámica freática en dos ambientes de la Pampa Interior con distintos regímenes de humedad. Cienc. del Suelo 33 (2) 263'272.
Forte Lay, J.A., Kruse, E., Aiello, J.L., 2007. Hydrologic scenarios applied to the agricultural management of the northwest of the Buenos Aires Province, Argentina. Geojournal 70 (4), 263–271.
Frenken, K., 2006. Technological innovation and complexity theory. Econ. Innovat. N. Technol. 15 (2), 137–155.
García, P.E., Badano, N., Menendez, A., Bert, F., García, G., Podestá, G., Rovere, S., Verdin, A., Balaji, R., Arora, P., 2018. Influencia de los cambios en el uso de suelo y las precipitaciones sobre la dinámica hídrica de una cuenca de llanura extensa. Caso de estudio: Cuenca del Río Salado, Buenos Aires, Argentina. Ribagua *in press*.
García, P.E., Menéndez, A.N., Podestá, G., Bert, F., Arora, P., Jobbágy, E., 2017. Land use as possible strategy for managing water table depth in flat basins with shallow groundwater. Int. J. River Basin Manag. 1–14.
Gilbert, N., 2008. Agent-based Models. SAGE, Los Angeles, CA.
Gotts, N.M., Polhill, J.G., 2009. When and how to imitate your neighbours: lessons from and for FEARLUS. J. Artif. Soc. Soc. Simulat. 12 (3), 2.
Gotts, N.M., Polhill, J.G., Law, A.N.R., Izquierdo, L.R., 2003. Dynamics of Imitation in a Land Use Simulation, Second International Symposium on Imitation in Animals and Artefacts. University of Wales, Aberystwyth, UK, pp. 39–46.
Grassini, P., Hall, A.J., Mercau, J.L., 2009. Benchmarking sunflower water productivity in semiarid environments. Field Crop. Res. 110 (3), 251–262.
Grimm, V., Railsback, S.F., 2005. Individual-based Modeling and Ecology. Princeton University Press, Princeton.
Grimm, V., Revilla, E., Berger, U., Jeltsch, F., Mooij, W.M., Railsback, S.F., Thulke, H.-H., Weiner, J., Wiegand, T., DeAngelis, D.L., 2005. Pattern-oriented modeling of agent-based complex systems: lessons from ecology. Science 310, 987–991.
Halcrow, Partners, 1999. Plan Maestro Integral de la Cuenca de Río Salado. Ministerio de Obras y Servicios Públicos de la Provincia de Buenos Aires, La Plata, Argentina.
Hall, A.J., Rebella, C.M., Ghersa, C.M., Culot, J.P., 1992. Field-corp systems of the pampas. In: Pearson, C.J. (Ed.), Field Crop Ecosystems: Ecosystems of the World. Elsevier, Amsterdam, Holland, pp. 413–450.
Haylock, M.R., Peterson, M.C., Alves, L.M., Ambrizzi, T., Anunção, Y.M.T., Baez, J., Barros, V.R., Berlato, M.A., Bidegain, M., Coronel, G., Corradi, V., Garcia, V.J., Grimm, A.M., Karoly, D., Marengo, J.A., Marino, M.B., Moncunill, D.F., Nechet, D., Quintana, J., Rebello, E., Rusticucci, M., Santos, J.L., Trebejo, I., Vincent, L.A., 2006. Trends in total and extreme south American rainfall in 1960–2000 and links with sea surface temperature. J. Clim. 19, 1490–1512.
Herriott, S.R., Levinthal, D., March, J.G., 1985. Learning from experience in organizations. Am. Econ. Rev. 75 (2), 298–302.
Herzer, H., 2003. Flooding in the pampean region of Argentina: the Salado Basin. In: Kreimer, A., Arnold, M., Carlin, A. (Eds.), Building Safer Cities: the Future of Disaster Risk. Disaster Risk Management Series. The World Bank, Disaster Management Facility: Washington DC, USA, pp. 137–147.
INTA, 1990. Atlas de Suelos de la República Argentina. Escala 1:500.000 y 1:1.000.000. CIRN. Instituto de Evaluación de Tierras, Buenos Aires, Argentina.
Jobbágy, E.G., Jackson, R.B., 2004. Groundwater use and salinization with grassland afforestation. Global Change Biol. 10, 1299–1312.
Jobbágy, E.G., Nosetto, M.D., Santoni, C.S., Baldi, G., 2008. El desafío ecohidrológico de las transiciones entre sistemas leñosos y herbáceos en la llanura Chaco-Pampeana. Ecol. Austral 18, 305–322.
Jones, J.W., Hoogenboom, G., Porter, C.H., Boote, K.J., Batchelor, W.D., Hunt, L.A., Wilkens, P.W., Singh, U., Gijsman, A.J., Ritchie, J.T., 2003. The DSSAT cropping system model. Eur. J. Agron. 18 (3–4), 235–265.
Kahlown, M.A., Azam, M., 2002. Individual and combined effect of waterlogging and salinity on crop yields in the Indus basin. Irrigat. Drain. 51, 329–338.
Kirsten, J., 2010. The new landscape of global agriculture. Agric. Econ. 41 ix.
Kristensen, K.J., Jensen, S.E., 1975. A model for estimating actual evapotranspiration from potential evapotranspiration. Nord. Hydrol 6 (3), 170–188.
Kruse, E., Forte Lay, J.A., Aiello, J.L., Basualdo, A., Heinzenknecht, G., 2001. Hydrological processes on large flatlands: case study in the northwest region of Buenos Aires Province (Argentina). 267. IAHS-AISH Publication, pp. 531–535.
Kuppel, S., Houspanossian, J., Nosetto, M.D., Jobbágy, E.G., 2015. What does it take to flood the Pampas?: lessons from a decade of strong hydrological fluctuations. Water Resour. Res. 51 (4), 2937–2950.
Lamers, P., McCormick, K., Hilbert, J.A., 2008. The emerging liquid biofuel market in Argentina: implications for domestic demand and international trade. Energy Pol. 36 (4), 1479–1490.
Lant, T.K., 1992. Aspiration level adaptation: an empirical exploration. Manag. Sci. 38 (5), 623–643.
Lowry, C.S., Loheide, S.P., 2010. Groundwater-dependent vegetation: quantifying the groundwater subsidy. Water Resour. Res. 46 (6) (n/a-n/a).
Ma, L., Hoogenboom, G., Ahuja, L.R., Ascough Ii, J.C., Saseendran, S.A., 2006. Evaluation of the RZWQM-CERES-Maize hybrid model for maize production. Agric. Syst. 87 (3), 274–295.
Ma, L., Hoogenboom, G., Ahuja, L.R., Nielsen, D.C., Ascough, J.C.I., 2005. Development and evaluation of the RZWQM-CROPGRO hybrid model for soybean production. Agron. J. 97 (4), 1172–1182 2005.
Ma, L., Malone, R.W., Jaynes, D.B., Thorp, K.R., Ahuja, L.R., 2008. Simulated effects of nitrogen management and soil microbes on soil nitrogen balance and crop production. Soil Sci. Soc. Am. J. 72 (6), 1594–1603.
Manuel-Navarrete, D., Gallopín, G.C., Blanco, M., Díaz-Zorita, M., Ferraro, D.O., Herzer, H., Laterra, P., Murmis, M.R., Podestá, G.P., Rabinovich, J., Satorre, E.H., Torres, F., Viglizzo, E.F., 2009. Multi-causal and integrated assessment of sustainability: the case of agriculturization in the Argentine Pampas. Environ. Dev. Sustain. 11 (3), 621–638.
March, J.G., 1988. Variable risk preferences and adaptive aspirations. J. Econ. Behav. Organ. 9 (1), 5–24.
Matthews, R., Gilbert, N., Roach, A., Polhill, J., Gotts, N., 2007. Agent-based land-use models: a review of applications. Landsc. Ecol. 22 (10), 1447–1459.
Mejia, M.N., Madramootoo, C.A., Broughton, R.S., 2000. Influence of water table management on corn and soybean yields. Agric. Water Manag. 46 (1), 73–89.
Menéndez, Á.N., Badano, N., Lecertua, E., Re, F., Re, M., 2012. Evaluación de las inundaciones y las obras de drenaje de la Cuenca del Saldo (prov. Buenos Aires) mediante modelación numérica. Instituto Nacional del Agua, Ezeiza, Argentina, pp. 323.
Mercau, J.L., Dardanelli, J.L., Collino, D.J., Andriani, J.M., Irigoyen, A., Satorre, E.H., 2007. Predicting on-farm soybean yields in the pampas using CROPGRO-soybean. Field Crop. Res. 100 (2–3), 200–209.
Mercau, J.L., Nosetto, M.D., Bert, F., Giménez, R., Jobbágy, E.G., 2016. Shallow groundwater dynamics in the Pampas: climate, landscape and crop choice effects. Agric. Water Manag. 163, 159–168.
Monzon, J.P., Sadras, V.O., Abbate, P.A., Caviglia, O.P., 2007. Modelling management strategies for wheat–soybean double crops in the south-eastern Pampas. Field Crop. Res. 101 (1), 44–52.
Nosetto, M.D., Jobbágy, E.G., Brizuela, A.B., Jackson, R.B., 2012. The hydrologic consequences of land cover change in central Argentina. Agric. Ecosyst. Environ. 154, 2–11.
Nosetto, M.D., Jobbágy, E.G., Jackson, R.B., Sznaider, G.A., 2009. Reciprocal influence of crops and shallow ground water in sandy landscapes of the Inland Pampas. Field Crop. Res. 113 (2), 138–148.
Nosetto, M.D., Paez, R.A., Ballesteros, S.I., Jobbágy, E.G., 2015. Higher water-table levels and flooding risk under grain vs. livestock production systems in the subhumid plains of the Pampas. Agric. Ecosyst. Environ. 206, 60–70 0.
Pinto, P., Fernández Long, M.E., Piñeiro, G., 2017. Including cover crops during fallow periods for increasing ecosystem services: is it possible in croplands of Southern South America? Agric. Ecosyst. Environ. 248, 48–57.
Polhill, J.G., Sutherland, L.-A., Gotts, N.M., 2010. Using qualitative evidence to enhance

an agent-based modelling system for studying land use change. J. Artif. Soc. Soc. Simulat. 13 (2), 10.
Qaim, M., Traxler, G., 2005. Roundup Ready soybeans in Argentina: farm level and aggregate welfare effects. Agric. Econ. 32, 73–86.
Rand, W., Rust, R.T., 2011. Agent-based modeling in marketing: guidelines for rigor. Int. J. Res. Market. 28 (3), 181–193.
Refsgaard, J.C., Storm, B., 1995. MIKE SHE. In: Singh, V.P. (Ed.), Computer Models of Watershed Hydrology. Water Resources Publications, pp. 809–846.
Refsgaard, J.C., Storm, B., Clausen, T., 2010. Système Hydrologique Europeén (SHE): review and perspectives after 30 years development in distributed physically-based hydrological modelling. Nord. Hydrol 41 (5), 355–377.
Richardson, C.W., 1981. Stochastic simulation of daily precipitation, temperature, and solar radiation. Water Resour. Res. 17 (1), 182–190.
Rimski-Korsakov, H., Alvarez, C.R., Lavado, R.S., 2015. Cover crops in the agricultural systems of the Argentine Pampas. J. Soil Water Conserv. 70 (6), 134A–140A.
Riquier, J., Bramao, D.L., Corne, J.P., 1970. A New System of Soil Appraisal in Terms of Actual and Potential Productivity: Rome, Italy. pp. 38.
Rosegrant, M.W., Ringler, C., Zhu, T., 2009. Water for agriculture: maintaining food security under growing scarcity. Annu. Rev. Environ. Resour. 34 (1), 205–222.
Rovere, S.L., North, M.J., Podestá, G.P., Bert, F.E., 2016. Practical points for the software development of an agent-based model of a coupled human-natural system. IEEE Access 4, 4282–4298.
Rulli, M.C., Bellomi, D., Cazzoli, A., De Carolis, G., D'Odorico, P., 2016. The water-land-food nexus of first-generation biofuels. Sci. Rep. 6, 22521.
Rusticucci, M., Penalba, O., 2000. Interdecadal changes in the precipitation seasonal cycle over Southern South America and their relationshio with surface temperature. Clim. Res. 16, 1–15.
Sadras, V.O., Cassman, K.G.G., Grassini, P., Hall, A.J., Bastiaanssen, W.G.M., Laborte, A.G., Milne, A.E., Sileshi, G., Steduto, P., 2015. Yield Gap Analysis of Field Crops – Methods and Case Studies, FAO Water Reports No. 41. FAO, Rome, Italy.
Sahoo, G.B., Ray, C., De Carlo, E.H., 2006. Calibration and validation of a physically distributed hydrological model, MIKE SHE, to predict streamflow at high frequency in a flashy mountainous Hawaii stream. J. Hydrol. 327 (1–2), 94–109.
Satorre, E.H., 2011. Recent changes in pampean agriculture: possible new avenues in coping with global change challenges. In: Araus, J.L., Slafer, G.A. (Eds.), Crop Stress Management and Global Climate Change. CABI, Wallingford, UK, pp. 47–57.
Satorre, E.H., Menéndez, F., Tinghitella, G.A., Cavasassi, J.L., 2005. TRIGUERO: un sistema de apoyo a la fertilización nitrogenada de trigo. Convenio AACREA y Profertil S. A., software de aplicación agronómica, Buenos Aires, Argentina.
Scarpati, O.E., Spescha, L., Capriolo, A., 2002. Occurrence of severe floods in the Salado river basin, buenos Aires province, Argentina. Mitig. Adapt. Strategies Glob. Change 7 (3), 285–301.
Schipanski, M.E., Barbercheck, M., Douglas, M.R., Finney, D.M., Haider, K., Kaye, J.P., Kemanian, A.R., Mortensen, D.A., Ryan, M.R., Tooker, J., White, C., 2014. A framework for evaluating ecosystem services provided by cover crops in agroecosystems. Agric. Syst. 125, 12–22.
Schreinemachers, P., Berger, T., 2006. Land use decisions in developing countries and their representation in multi-agent systems. J. Land Use Sci. 1 (1), 29–44.
Seager, R., Naik, N., Baethgen, W., Robertson, A., Kushnir, Y., Nakamura, J., Jurburg, S., 2010. Tropical oceanic causes of interannual to multidecadal precipitation variability in southeast south America over the past century. J. Clim. 23 (20), 5517–5539.
Sinclair, T.R., Salado-Navarro, L.R., Salas, G., Purcell, L.C., 2007. Soybean yields and soil water status in Argentina: simulation analysis. Agric. Syst. 94 (2), 471–477.
Smith, E.G., Eiswerth, M.E., Veeman, T.S., 2010. Current and emerging water issues in agriculture: an overview. Can. J. Agri. Econ./Revue canadienne d'agroeconomie 58, 403–409.
SMN, 2017. Servicios Climáticos. Atlas Climático. Servicio Meteorológico Nacional, Buenos Aires, Argentina.
Trigo, E.J., Cap, E., Malach, V., Villarreal, F., 2009. The case of zero-tillage technology in Argentina, Discussion Paper. International Food Policy Research Institute.
Vargas, W.M., Minetti, J.L., Poblete, A.G., 2002. Low-frequency oscillations in climatic and hydrological variables in southern South America's tropical-subtropical regions. Theor. Appl. Climatol. 72 (1–2), 29–40.
Verburg, P.H., Overmars, K.P., 2009. Combining top-down and bottom-up dynamics in land use modeling: exploring the future of abandoned farmlands in Europe with the Dyna-CLUE model. Landsc. Ecol. 24 (9), 1167.
Verdin, A., Rajagopalan, B., Kleiber, W., Podestá, G., Bert, F., 2018. A conditional stochastic weather generator for seasonal to multi-decadal simulations. J. Hydrol. 556, 835–846.
Viglizzo, E.F., Frank, F.C., Carreño, L.V., Jobbágy, E.G., Pereyra, H., Clatt, J., Pincén, D., Ricard, M.F., 2011. Ecological and environmental footprint of 50 years of agricultural expansion in Argentina. Global Change Biol. 17 (2), 959–973.
Viglizzo, E.F., Jobbágy, E.G., Frank, F.C., Aragón, R., De Oro, L., Salvador, V., 2009. The dynamics of cultivation and floods in arable lands of Central Argentina. Hydrol. Earth Syst. Sci. 13, 491–502.
Viglizzo, E.F., Lértora, F., Pordomingo, A.J., Bernardos, J.N., Roberto, Z.E., Del Valle, H., 2001. Ecological lessons and applications from one century of low external-input farming in the pampas of Argentina. Agric. Ecosyst. Environ. 83 (1), 65–81.
Zipper, S.C., Soylu, M.E., Booth, E.G., Loheide, S.P., 2015. Untangling the effects of shallow groundwater and soil texture as drivers of subfield-scale yield variability. Water Resour. Res. 51 (8), 6338–6358.
Zipper, S.C., Soylu, M.E., Kucharik, C.J., Loheide Ii, S.P., 2017. Quantifying indirect groundwater-mediated effects of urbanization on agroecosystem productivity using MODFLOW-AgroIBIS (MAGI), a complete critical zone model. Ecol. Model. 359, 201–219.